COBEM 99
XV Congresso Brasileiro de Engenharia Mecânica
15th Brazilian Congress of Mechanical Engineering
22 - 26 de Novembro de 1999 / November 22 - 26, 1999 Águas de Lindóia, São Paulo,

A UNIFIED FORMULATION FOR COMPRESSIBLE AND NEARLY INCOMPRESSIBLE VISCOUS FLOWS

Paulo A. B. de Sampaio
Maria de Lourdes Moreira
Instituto de Engenharia Nuclear - CNEN
Cx. P. 68550 - 21945-970 - Rio de Janeiro, RJ, Brazil

Abstract. *A unified formulation for both compressible and nearly incompressible viscous flow is presented. The new method is a subtle but relevant modification to the authors' previous formulation for all speed flow. The new discretised equations assume a simpler form, leading to an easier and more efficient computer implementation. The main features remain the same: the use of a segregated scheme, the choice of mass-velocity (density*velocity), internal energy and pressure as dependent variables, and the introduction of a strongly implicit pressure equation. The method is applied to the analysis of laminar flows governed by the Navier-Stokes equations. Computations of transonic and supersonic viscous flows around a Naca0012 airfoil are presented.*

Keywords: *Computational Fluid Dynamics, Aerodynamics, Adaptive Methods.*

1. INTRODUCTION

Most numerical methods for compressible fluid dynamics present difficulties when applied to low speed (nearly incompressible) flows. The difficulties originate from the fast propagation of pressure waves, as flow conditions approach the incompressible limit. Nearly incompressible flows, i.e. flows characterised by very small Mach number, are usually approximated as fully incompressible. Thus, compressibility effects are eliminated at the modelling level, prior to considering any particular discretisation method. In such a context, pressure is no longer a thermodynamic property related to density through a state equation. Most importantly, the pressure hyperbolic character and the associated wavelike propagation disappear from the model. Instead, pressure takes an elliptic character and must be determined from the momentum balance and boundary conditions, in such a way that a solenoidal velocity field is enforced.

In view of such physical and mathematical differences, it is not surprising that methods for the discretisation of compressible and incompressible flows have developed independently. The CFD literature reflects this dichotomy and most papers are devoted specifically to either compressible or incompressible applications. Nevertheless, the development of methods for a wide range of Mach number is important to the analysis of many flow problems involving simultaneously both the compressible and the nearly incompressible behaviour. In fact, even in the high-speed compressible flows of the aerospace

industry, the nearly incompressible behaviour is present near solid walls and leading edges, where the local fluid velocity is small compared to the local sound speed.

Different approaches have been pursued in the development of methods for all speed fluid flow. Karki & Patankar (1989) and Maliska & Silva (1989) introduced finite-volume pressure based methods obtained through the extension of schemes originally developed for incompressible problems. The works of Chen & Pletcher (1991) and Azevedo & Martins (1993) are examples of classical finite-volume compressible methods modified in order to deal with incompressible flows. In the finite element context, Zienkiewicz & Codina (1995) used fractional steps and characteristic-Galerkin approximations to derive their all speed formulation.

This paper presents a unified treatment for both compressible and nearly incompressible problems. The method is a subtle but relevant modification to our previous formulation for all speed flow (De Sampaio & Moreira, 1998) and (Moreira, 1998), leading to a simpler computer implementation. An important feature of the method is the implicit time discretisation of the mass balance and of the pressure terms appearing in the momentum and energy equations. Petrov-Galerkin weighting functions, derived from a least-squares approximation, are employed in the momentum and energy weighted residual statements. The resulting formulation automatically introduces streamline upwinding and pressure stabilising terms.

A segregated solution algorithm is employed. Once the pressure field is found, the scheme proceeds with the computation of the mass-velocity (density*velocity) and internal energy fields. The cyclic update of pressure, mass-velocity and internal energy requires the solution of symmetric systems of equations. This is accomplished using a preconditioned conjugate gradient solver.

The method is applied to the analysis of laminar flows governed by the Navier-Stokes equations. Computations of transonic and supersonic viscous flows around a Naca0012 airfoil are presented.

2. GOVERNING EQUATIONS

The equations for conservation of mass, momentum and energy are defined on the open bounded domain Ω, with boundary Γ, contained in the *nsd*-dimensional space. For *a =1,...,nsd* and *b=1,...,nsd*, the governing equations can be written in Cartesian co-ordinates as follows:

$$\frac{\partial \rho}{\partial t} + \frac{\partial G_a}{\partial x_a} = 0 \tag{1}$$

$$\frac{\partial G_a}{\partial t} + u_b \frac{\partial G_a}{\partial x_b} + \frac{\partial u_b}{\partial x_b} G_a - \frac{\partial \tau_{ab}}{\partial x_b} + \frac{\partial p}{\partial x_a} - \rho g_a = 0 \tag{2}$$

$$\rho \left(\frac{\partial e}{\partial t} + u_b \frac{\partial e}{\partial x_b} \right) + p \frac{\partial u_b}{\partial x_b} + \frac{\partial q_b}{\partial x_b} - \tau_{ab} \frac{\partial u_a}{\partial x_b} = 0 \tag{3}$$

The constitutive equations for viscous stress and heat-flux are, respectively,

$$\tau_{ab} = -\frac{2}{3} \mu \left(\frac{\partial u_c}{\partial x_c} \right) \delta_{ab} + \mu \left(\frac{\partial u_a}{\partial x_b} + \frac{\partial u_b}{\partial x_a} \right) \tag{4}$$

$$q_b = -\kappa \frac{\partial T}{\partial x_b} \tag{5}$$

The model is closed specifying a state equation for the fluid. The state equation for an ideal gas is assumed in this work,

$$p = (\gamma - 1)\rho e \tag{6}$$

where $\gamma = c_p / c_v$ and $e = c_v T$.

In the above equations u_a, p, e, ρ and T denote the velocity, pressure, internal energy, density and temperature fields, respectively. The mass-velocity (density*velocity) is represented by $G_a = \rho u_a$. The gravity field is g_a. The symbols μ, κ, c_v and c_p represent the fluid properties of viscosity, thermal conductivity, specific heat at constant volume and specific heat at constant pressure, respectively.

Note that the equations above are written in dimensional form and include density as dependent variable in the balance of mass. However, in order to derive a method suitable for a wide range of Mach number, we decided to introduce pressure as a main dependent variable instead. Thus, the state equation is used to eliminate density from the mass balance, replacing it by pressure and internal energy. As we shall see, this will permit the derivation of a strongly implicit pressure equation, which is of foremost importance in regions of low Mach number.

Let us define non-dimensional variables, denoted by the superscript '*', which are related to the original dimensional variables according to

$$\begin{array}{llll} u_a^* = u_a / u_0 & p^* = (p - p_0 - \rho_0 g_b x_b)/\rho_0 u_0^2 & T^* = (T - T_0)/T_0 & \\ \rho^* = \rho/\rho_0 & G_b^* = G_b / \rho_0 u_0 & e^* = (e - e_0)/e_0 & g_a^* = g_a / \|\mathbf{g}\| \\ \mu^* = \mu / \mu_0 & \kappa^* = \kappa / \kappa_0 & x_a^* = x_a / L & t^* = u_0 t / L \end{array} \tag{7}$$

where the subscript '$_0$' indicates reference values and L is the reference length. In terms of the non-dimensional variables, the governing equations can be written:

$$\alpha^* \frac{\partial p^*}{\partial t^*} - \beta^* \frac{\partial e^*}{\partial t^*} + \frac{\partial G_a^*}{\partial x_a^*} = 0 \tag{8}$$

$$\frac{\partial G_a^*}{\partial t^*} + u_b^* \frac{\partial G_a^*}{\partial x_b^*} + \frac{\partial u_b^*}{\partial x_b^*} G_a^* - \frac{1}{R_e} \frac{\partial \tau_{ab}^*}{\partial x_b^*} + \frac{\partial p^*}{\partial x_a^*} - \frac{1}{F_r^2} (\rho^* - 1) g_a^* = 0 \tag{9}$$

$$\rho^* \left(\frac{\partial e^*}{\partial t^*} + u_b^* \frac{\partial e^*}{\partial x_b^*} \right) + \left(\gamma - 1 + \gamma E_c p^* - \frac{\gamma E_c}{F_r^2} \varphi^* \right) \frac{\partial u_b^*}{\partial x_b^*} + \frac{\gamma}{R_e P_r} \frac{\partial q_b^*}{\partial x_b^*} - \frac{\gamma E_c}{R_e} \tau_{ab}^* \frac{\partial u_a^*}{\partial x_b^*} = 0 \tag{10}$$

Note that using the mass balance and the state equation, the energy equation (10) can be alternatively written as

$$\gamma \rho^* \left(\frac{\partial e^*}{\partial t^*} + u_b^* \frac{\partial e^*}{\partial x_b^*} \right) + \frac{\gamma}{R_e P_r} \frac{\partial q_b^*}{\partial x_b^*} - \frac{\gamma E_c}{R_e} \tau_{ab}^* \frac{\partial u_a^*}{\partial x_b^*} = \gamma E_c \left[\frac{\partial p^*}{\partial t^*} + u_b^* \frac{\partial p^*}{\partial x_b^*} + \frac{1}{F_r^2} u_b^* g_b^* \right] \tag{11}$$

The constitutive equations for viscous stress and heat flux, and the equation of state, take the following non-dimensional forms, respectively,

$$\tau^*_{ab} = -\frac{2}{3}\mu^*\left(\frac{\partial u^*_c}{\partial x^*_c}\right)\delta_{ab} + \mu^*\left(\frac{\partial u^*_a}{\partial x^*_b} + \frac{\partial u^*_b}{\partial x^*_a}\right) \tag{12}$$

$$q^*_b = -\kappa^*\frac{\partial T^*}{\partial x^*_b} \tag{13}$$

$$\rho^* = \frac{\left(\gamma - 1 + \gamma E_c\, p^* - \dfrac{\gamma E_c}{F_r^2}\varphi^*\right)}{(\gamma - 1)\left(e^* + 1\right)} \tag{14}$$

We have also introduced the non-dimensionalised thermodynamic properties $\alpha^* = u_0^2\,(\partial\rho/\partial p)_e$ and $\beta^* = e_0(\partial\rho/\partial e)_p/\rho_0$, and the non-dimensionalised gravity field potential $\varphi^* = -g_a\, x_a / \|\mathbf{g}\| L$. The non-dimensional groups of Reynolds, Froude, Prandtl and Eckert are given by

$$R_e = \frac{\rho_0\, u_0\, L}{\mu_0} \qquad F_r = \frac{u_0}{\sqrt{\|\mathbf{g}\| L}} \qquad P_r = \frac{\mu_0\, c_p}{\kappa_0} \qquad E_c = \frac{u_0^2}{c_p\, T_0} \tag{15}$$

In aeronautical applications it is usual to parameterise problems using the Mach number M rather than the Eckert number E_c. For ideal gases the relationship between these non-dimensional groups is $E_c = (\gamma - 1)M^2$.

The non-dimensionalised equations presented above are slightly different from those originally shown in (De Sampaio & Moreira, 1998) and (Moreira, 1998). The difference arises from a new definition of the non-dimensional modified pressure p^*. The equations presented here take a simpler form, leading to a more efficient computer implementation.

In the remainder of this work we shall deal exclusively with the non-dimensionalised equations and the superscript '*' will be dropped.

3. THE DISCRETISATION AND SOLUTION SCHEMES

Linear Lagrangian finite elements are employed to represent the mass-velocity, pressure and internal energy fields. The central feature of the method is the derivation of a discretised equation for pressure, where pressure contributions arising from the mass, momentum and energy balances are taken implicitly in the time-discretisation. The Galerkin method is used to obtain the discretised pressure equation, whilst a Petrov-Galerkin / least-squares based approach is used in the derivation of the discretised equations for mass-velocity and internal energy. The problem is solved using a segregated solution procedure. Once the pressure field is found, the algorithm proceeds with the computation of the mass-velocity and internal energy fields. The cyclic update of pressure, mass-velocity and internal energy requires the solution of symmetric systems of equations. This is accomplished with preconditioned conjugate gradient solvers, suitable for parallel/vector implementation in supercomputers (De Sampaio & Coutinho, 1999).

3.1 The strongly implicit pressure equation

Let us consider the following time-discretisation of the mass balance Eq. (8),

$$\alpha^n\left(\frac{p^{n+1}-p^n}{\Delta t}\right)-\frac{\beta^n}{\rho^{n+1/2}}\left[\rho^{n+1/2}\left(\frac{e^{n+1}-e'}{\Delta t}\right)\right]+\frac{\partial G_a^{n+1}}{\partial x_a}\quad=\frac{\beta^n}{\rho^{n+1/2}}\left[\rho^{n+1/2}\left(\frac{e'-e^n}{\Delta t}\right)\right] \tag{16}$$

and the fractional steps approximation of the energy balance Eq. (10), represented by

$$\rho^{n+1/2}\left(\frac{e'-e^n}{\Delta t}+\theta_1\ u_b^n\frac{\partial e'}{\partial x_b}+\theta_2\ u_b^n\frac{\partial e^n}{\partial x_b}\right)+\frac{\gamma}{R_eP_r}\frac{\partial q_b^n}{\partial x_b}-\frac{\gamma E_c}{R_e}\tau_{ab}^n\frac{\partial u_a^n}{\partial x_b}=0 \tag{17}$$

$$\rho^{n+1/2}\left(\frac{e^{n+1}-e'}{\Delta t}\right)+\left(\gamma-1+\gamma E_c\,p^{n+1}-\frac{\gamma E_c}{F_r^2}\varphi\right)\frac{\partial u_b^n}{\partial x_b}=0 \tag{18}$$

In the above equations, the superscripts n and $n+1$ denote the time-level and Δt is the time-step. Here, the parameters θ_1 and $\theta_2=1-\theta_1$ control the implicitness in the time discretisation of the convective term (explicit for $\theta_1=0$ and implicit for $\theta_1=1$). Unless otherwise stated, we shall employ $\theta_1=0.5$ in our computations. The mass-velocity, pressure and internal energy fields at time-level k are interpolated as $\hat{G}_a^k=N_jG_{aj}^k$, $\hat{p}^k=N_jp_j^k$ and $\hat{e}^k=N_je_j^k$, respectively, where N_j represents the linear Lagrangian shape functions and G_{aj}^k, p_j^k and e_j^k are the corresponding nodal values at time-level k. The thermodynamic properties ρ^n, α^n and β^n are evaluated as constants within each finite element (they are obtained from the internal energy and pressure defined at the element baricentre). The density $\rho^{n+1/2}$, also approximated as constant within each element, is computed using a Taylor series expansion from time-level n and the balance of mass,

$$\rho^{n+1/2}=\rho^n+\frac{\Delta t}{2}\frac{\partial\ \rho^n}{\partial\ t}\ =\ \rho^n-\frac{\Delta t}{2}\frac{\partial\hat{G}_a^n}{\partial x_a} \tag{19}$$

Note that when splitting the energy balance into equations Eq.(17) and Eq.(18), we have isolated the term representing the compressible contribution in Eq.(18). Equation (17), on the other hand, retains the remaining terms, typical of incompressible applications. Substituting Eq.(18) into the mass balance Eq.(16), we obtain

$$\alpha^n\left(\frac{p^{n+1}-p^n}{\Delta t}\right)+\frac{\beta^n}{\rho^{n+1/2}}\left[\gamma-1+\gamma E_c\,p^{n+1}-\frac{\gamma E_c}{F_r^2}\varphi\right]\frac{\partial u_a^n}{\partial x_a}+\frac{\partial G_a^{n+1}}{\partial x_a}=$$
$$\frac{\beta^n}{\rho^{n+1/2}}\left[\rho^{n+1/2}\left(\frac{e'-e^n}{\Delta t}\right)\right] \tag{20}$$

The strongly implicit pressure equation is derived using the Galerkin method to approximate the above equation, where the momentum balance is employed to express G_a^{n+1}

in terms of the various forces acting on the fluid. In particular, the pressure gradient contribution to the momentum balance is taken at time level *n+1*. The name strongly implicit pressure equation derives from the fact that the pressure terms arising from the mass, momentum and energy balances are approximated using an implicit time-discretisation. This introduces damping of pressure errors and permits retaining stability in the pressure computation, despite ignoring the short time-scales associated to the fast pressure waves that characterise nearly incompressible flows.

In the strongly implicit pressure equation below, the weighting functions N_i are the shape functions associated to free nodal pressure variables p_i^{n+1}. The boundary conditions considered are pressure and mass flux. These are prescribed on non-overlapping parts of the boundary Γ_p and Γ_G, such that $p = \bar{p}$ on Γ_p and $G_a\, n_a = \bar{G}$ on Γ_G.

$$
\begin{aligned}
&\int_\Omega N_i \left(\frac{\alpha^n}{\Delta t} + \frac{\gamma E_c \beta^n}{\rho^{n+1/2}} \frac{\partial \hat{u}_b^n}{\partial x_b} \right) \hat{p}^{n+1} d\Omega \;+\; \int_\Omega \Delta t \; \frac{\partial N_i}{\partial x_a} \frac{\partial \hat{p}^{n+1}}{\partial x_a} d\Omega = \int_\Omega N_i \frac{\alpha^n}{\Delta t} \hat{p}^n \, d\Omega \\
&+ \int_\Omega N_i \frac{\beta^n}{\Delta t} \left(\hat{e}' - \hat{e}^n \right) d\Omega + \int_\Omega \Delta t \, \frac{1}{F_r^2} \left(\rho^{n+1/2} - 1 \right) \frac{\partial N_i}{\partial x_a} g_a \; d\Omega - \int_\Omega N_i \frac{\partial \hat{G}_a^n}{\partial x_a} d\Omega \\
&- \int_\Omega \Delta t \frac{\partial N_i}{\partial x_a} \left(\hat{u}_b^n \frac{\partial \hat{G}_a^n}{\partial x_b} + \frac{\partial u_b^n}{\partial x_b} \hat{G}_a^n \right) d\Omega \;+ \int_\Omega N_i \left(\frac{\gamma E_c}{F_r^2} \varphi + 1 - \gamma \right) \frac{\beta^n}{\rho^{n+1/2}} \frac{\partial \hat{u}_a^n}{\partial x_a} d\Omega \\
&- \int_{\Gamma_G} N_i \left(\bar{G}^{n+1} - \bar{G}^n \right) d\Gamma \qquad\qquad \forall \;\; free \;\; p_i^{n+1}
\end{aligned}
\tag{21}
$$

3.2. Petrov-Galerkin / least-squares based discretisations

It is important to note that before Eq.(21) can be solved, one has to determine the internal energy field $\hat{e}'$ corresponding to the solution of Eq.(17). A Petrov-Galerkin / least-squares based weighted residual method is applied to that end. Boundary conditions are internal energy and heat-flux. These are prescribed on non-overlapping parts of the boundary Γ_e and Γ_q, such that $e' = \bar{e}$ on Γ_e and $q_b\, n_b = \bar{q}$ on Γ_q. The resulting discretised equation is

$$
\begin{aligned}
&\int_\Omega \left(N_i + \theta_1 \, \Delta t \; \hat{u}_c^n \frac{\partial N_i}{\partial x_c} \right) \frac{\hat{\rho}^{n+1/2}}{\Delta t} \left(\hat{e}' + \theta_1 \, \Delta t \; \hat{u}_b^n \frac{\partial \hat{e}'}{\partial x_b} \right) d\Omega \;= \\
&\int_\Omega \left(N_i + \theta_1 \, \Delta t \; \hat{u}_c^n \frac{\partial N_i}{\partial x_c} \right) \frac{\hat{\rho}^{n+1/2}}{\Delta t} \left(\hat{e}^n - \theta_2 \, \Delta t \; \hat{u}_b^n \frac{\partial \hat{e}^n}{\partial x_b} \right) d\Omega \;+ \\
&\int_\Omega \left(N_i + \theta_1 \, \Delta t \; \hat{u}_c^n \frac{\partial N_i}{\partial x_c} \right) \frac{\gamma \, E_c}{R_e} \; \hat{\tau}_{ab}^n \; \frac{\partial \hat{u}_a^n}{\partial x_b} \; d\Omega \;+ \int_\Omega \frac{\gamma}{R_e \, P_r} \frac{\partial N_i}{\partial x_b} \hat{q}_b^n \; d\Omega \\
&- \int_{\Gamma_q} \frac{\gamma}{R_e \, P_r} N_i \, \bar{q} \; d\Gamma - \int_\Omega \; \theta_1 \, \Delta t \; \hat{u}_c^n \frac{\partial N_i}{\partial x_c} \frac{\gamma}{R_e P_r} \frac{\partial \hat{q}_b^n}{\partial x_b} d\Omega \qquad \forall \;\; free \;\; e_i'
\end{aligned}
\tag{22}
$$

The Petrov-Galerkin / least-squares based weighted residual method is also used to update the mass-velocity G_a^{n+1}. Mass-velocity and traction boundary conditions are specified on Γ_{Ga} and Γ_{ta}, such that $G_a = \bar{G}_a$ on Γ_{Ga} and $\left(-p \;\; \delta_{ab} + \tau_{ab} / R_e \right) n_b = \bar{t}_a$ on Γ_{ta}. The resulting discretised equation is

$$\int_\Omega \left[\left(1+\theta_1\,\Delta t\frac{\partial \hat{u}_c^n}{\partial x_c}\right)N_i+\theta_1\,\Delta t\,\hat{u}_c^n\frac{\partial N_i}{\partial x_c}\right]\frac{1}{\Delta t}\left[\left(1+\theta_1\;\Delta t\frac{\partial \hat{u}_b^n}{\partial x_b}\right)\hat{G}_a^{n+1}+\theta_1\;\Delta t\,\hat{u}_b^n\frac{\partial \hat{G}_a^{n+1}}{\partial x_b}\right]d\Omega=$$
$$\int_\Omega \left[\left(1+\theta_1\,\Delta t\frac{\partial \hat{u}_c^n}{\partial x_c}\right)N_i+\theta_1\,\Delta t\,\hat{u}_c^n\frac{\partial N_i}{\partial x_c}\right]\frac{1}{\Delta t}\left[\left(1-\theta_2\;\Delta t\frac{\partial \hat{u}_b^n}{\partial x_b}\right)\hat{G}_a^{n}-\theta_2\;\Delta t\,\hat{u}_b^n\frac{\partial \hat{G}_a^{n}}{\partial x_b}\right]d\Omega\;+$$
$$\int_\Omega \theta_1\,\Delta t\left[\frac{\partial \hat{u}_c^n}{\partial x_c}N_i+\;\hat{u}_c^n\frac{\partial N_i}{\partial x_c}\right]\left[\frac{1}{R_e}\frac{\partial \hat{\tau}_{ab}^n}{\partial x_b}-\frac{\partial \hat{p}^{n+1}}{\partial x_a}\right]d\Omega-\int_\Omega\frac{\partial N_i}{\partial x_b}\left(-\hat{p}^{n+1}\delta_{ab}+\frac{\hat{\tau}_{ab}^n}{R_e}\right)d\Omega\;+$$
$$\int_\Omega \left[\left(1+\theta_1\;\Delta t\frac{\partial \hat{u}_c^n}{\partial x_c}\right)N_i+\;\theta_1\,\Delta t\,\hat{u}_c^n\frac{\partial N_i}{\partial x_c}\right]\left[\frac{1}{F_r^2}\left(\hat{\rho}^{n+1/2}-1\right)g_a\right]d\Omega\;+\int_{\Gamma_{t\sigma}}N_i\,\bar{t}_a\;d\Gamma$$
$$\forall\ free\ G_{ai}^{n+1} \qquad (23)$$

The final step of the segregated solution procedure is the computation of the new internal energy field $\hat{e}^{n+1}$. The Petrov-Galerkin / least-squares based weighted residual method is applied to approximate the energy equation Eq.(11). After introducing the prescribed internal energy and heat-flux boundary conditions, we obtain:

$$\int_\Omega\left(N_i+\theta_1\,\Delta t\,\hat{u}_c^n\frac{\partial N_i}{\partial x_c}\right)\gamma\frac{\hat{\rho}^{n+1/2}}{\Delta t}\left(\hat{e}^{n+1}+\theta_1\;\Delta t\,\hat{u}_b^n\frac{\partial \hat{e}^{n+1}}{\partial x_b}\right)d\Omega\;=$$
$$\int_\Omega\left(N_i+\theta_1\,\Delta t\,\hat{u}_c^n\frac{\partial N_i}{\partial x_c}\right)\gamma\frac{\hat{\rho}^{n+1/2}}{\Delta t}\left(\hat{e}^{n}-\theta_2\;\Delta t\,\hat{u}_b^n\frac{\partial \hat{e}^{n}}{\partial x_b}\right)d\Omega\;+$$
$$\int_\Omega\frac{\gamma}{R_eP_r}\frac{\partial N_i}{\partial x_b}\hat{q}_b^n\;d\Omega-\int_{\Gamma_q}\frac{\gamma}{R_eP_r}N_i\,\bar{q}\;d\Gamma-\int_\Omega\frac{\gamma}{R_eP_r}\;\theta_1\,\Delta t\,\hat{u}_c^n\frac{\partial N_i}{\partial x_c}\frac{\partial \hat{q}_b^n}{\partial x_b}\;d\Omega\;+$$
$$\int_\Omega\left(N_i+\theta_1\;\Delta t\,\hat{u}_c^n\frac{\partial N_i}{\partial x_c}\right)\gamma E_c\left[\frac{\hat{p}^{n+1}-\hat{p}^n}{\Delta t}+\hat{u}_b^n\frac{\partial \hat{p}^{n+1}}{\partial x_b}+\frac{1}{F_r^2}\hat{u}_b^n\,g_b+\frac{1}{R_e}\hat{\tau}_{ab}^n\frac{\partial \hat{u}_a^n}{\partial x_b}\right]d\Omega$$
$$\forall\ free\ e_i^{n+1} \qquad (24)$$

3.3 The time-space adaptive procedure

When dealing with transient problems, the overall error in the solution is associated not only to the spatial discretisation, but also to the time integration of the governing equations. In this work we combine a remeshing scheme with the local time-stepping algorithm introduced by De Sampaio (1993). This algorithm sets local time-steps based on the time-scales of the convection-diffusion processes resolvable on a given mesh. These time-scales are estimated according to local values of velocity and physical properties, and according to the local mesh resolution.

The *a posteriori* error estimator proposed by Zienkiewicz & Zhu (1987) is used to estimate the velocity gradient error and to guide the remeshing. The scheme is designed to generate meshes containing a controlled number of elements, in such a way that the velocity gradient error becomes evenly distributed. The remeshing procedure is fully automatic and triggered during a transient analysis, whenever the relative variation of the estimated error exceeds a preset value.

The local time-stepping algorithm is used in conjunction with the remeshing scheme. This permits linking spatial and time-step refinement and naturally leads to a simultaneous

time-space adaptive procedure. Indeed, whenever the remeshing scheme creates some local refinement to better resolve a particular flow feature, the time-step distribution is also adapted accordingly, so that the corresponding time evolution can be appropriately followed.

4. NUMERICAL EXAMPLES

The formulation presented in the previous sections has been applied to the analysis of transonic and supersonic viscous flows around a Naca0012 airfoil. The reference properties and the reference velocity used for non-dimensionalising the problems are those corresponding to the free stream. The airfoil chord is chosen as the characteristic length L.

Note that due to the presence of boundary layers, these flows involve a wide range of Mach number. In the supersonic example, for instance, the local Mach number ranges from zero (at the airfoil surface) to more than 2. The thermodynamic and transport properties of air were used in the examples. Air viscosity was determined using Sutherland's formula (Hirsch, 1988). A constant Prandtl number of 0.72 was assumed throughout.

The first example is a transonic flow with M=0.85, Re=500 and 0^0 incidence. A fixed mesh, refined close to the airfoil surface, was used. The mesh contains 5328 nodes and 10238 elements. Mass-velocity and temperature are imposed at the inflow boundary whilst pressure is imposed at the outflow. At the airfoil surface the no-slip velocity condition is applied together with a uniform temperature corresponding to the free stream stagnation value.

Figure 1 shows the mesh employed and the friction coefficient along the chord. The result obtained is in good agreement with the friction coefficient presented by Nigro *et al.* (1997).

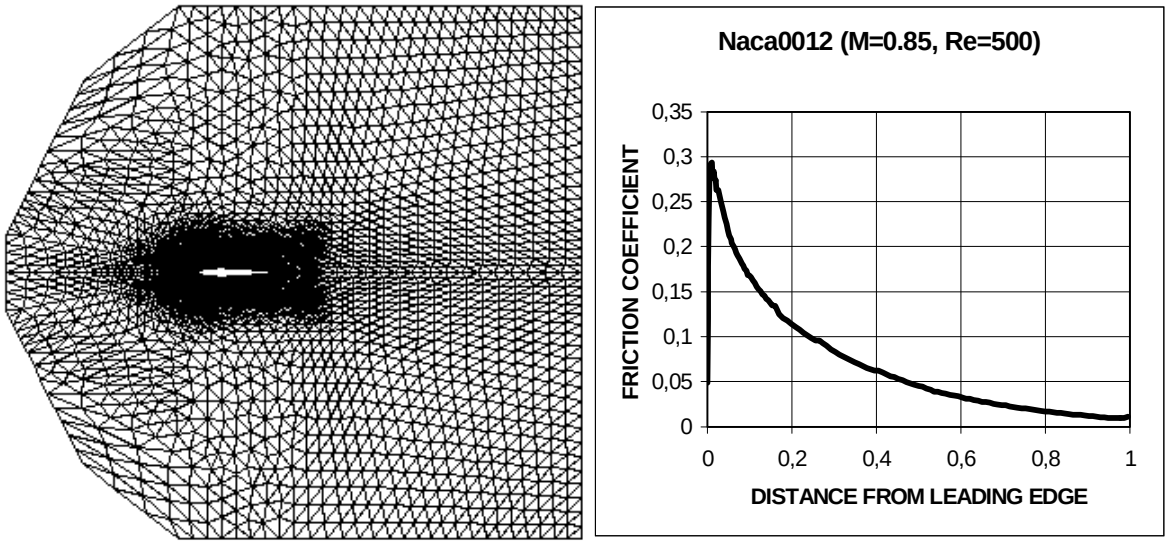

Figure 1- Mesh and friction coefficient for a transonic flow around a Naca0012 airfoil.

The second example is a supersonic flow at M=2.0, Re=106 and 10^0 incidence. Here, mass-velocity, temperature and pressure are imposed at the supersonic inflow boundary. The no-slip velocity condition is applied at the airfoil surface, which is assumed adiabatic. No boundary conditions are imposed at the supersonic outflow. In this example, we have performed a transient, time-space adaptive computation. The remeshing procedure was employed to construct meshes according to the estimated error on velocity gradients, whilst local time-steps were adjusted according to the resulting element sizes and physical conditions.

The transient was run from $t^* = 0$ to $t^* = 10$. At $t^* = 10$ the computation is virtually at steady state, with a residual of 0.001. Figure 2 shows a detail of the final adaptive mesh (11318 nodes, 22205 elements), together with density and Mach number contours. In particular, note the refinement on the frontal shock and boundary layer.

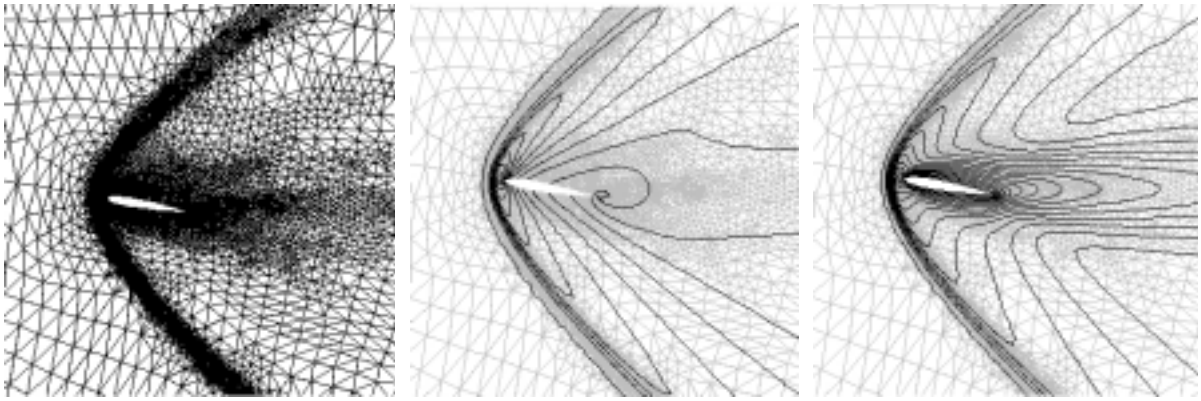

Mesh Density Mach

Figure 2- Supersonic flow around a Naca0012 airfoil.

Figure 3 presents a comparison between the computed density field and the corresponding experimental data obtained by Allègre *et al.* (1987). The comparison is made on the straight line AB, which runs through the shock into the rarefaction zone. Note the good agreement between the numerical and the experimental density data.

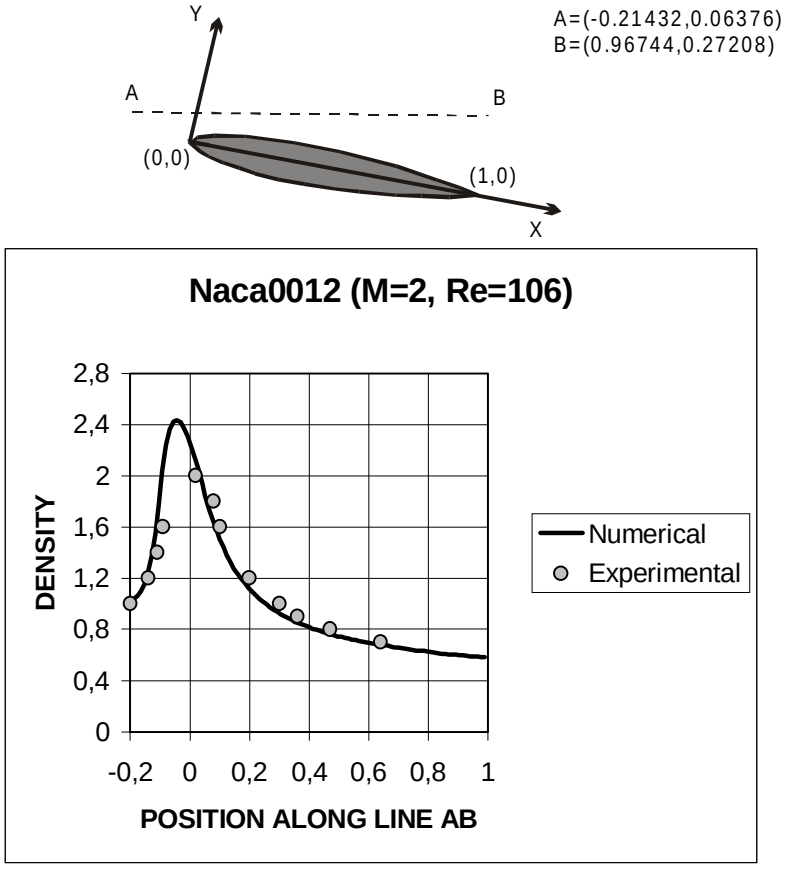

Figure 3- Comparison between experimental and computed density data.

5. CONCLUDING REMARKS

A finite element formulation designed for the analysis of both compressible and nearly incompressible fluid dynamics has been presented. The method is a subtle but relevant modification to our previous formulation for all speed flow, leading to a simpler computer implementation. The examples shown, involving a wide variation of Mach number, demonstrate the effectiveness of the new formulation.

The numerical methods presented herein for 2D laminar flows naturally extend for the study of 3D problems. Extensions to turbulent analyses are also possible, using either Reynolds averaged equations or LES procedures.

REFERENCES

Allègre, J., Raffin, M. & Lengrand, J.C., 1987, Experimental flowfields around Naca0012 airfoils located in subsonic and supersonic rarefied air streams, in Numerical Simulation of Compressible Navier-Stokes Flows, a GAMM-Workshop, Notes on Numerical Fluid Dynamics, eds. M. O. Bristeau, R. Glowinski, J. Periaux and H. Viviand, Vol. 18.

Azevedo, J.L.F. & Martins, R.J., 1993, Compressible and incompressible flow simulations using a finite difference method, Proceedings of the 5th International Symposium on Computational Fluid Dynamics, Sendai, Japan, pp. 38-43.

Chen K.H. & Pletcher, R.H., 1991, Primitive variable, strongly implicit calculation procedure for viscous flows at all speeds, AIAA Journal, vol. 29, pp. 1241-1249, 1991.

De Sampaio, P.A.B., 1993, Transient solutions of the incompressible Navier-Stokes equations in primitive variables employing optimal local time-stepping, in Numerical Methods in Laminar and Turbulent Flow 1993, ed. C. Taylor, Pineridge Press, Swansea.

De Sampaio, P.A.B. & Moreira, M.L., 1998, A new finite element formulation for both compressible and nearly incompressible fluid dynamics, CT IEN/SUTER 02/98 (also accepted by the International Journal for Numerical Methods in Fluids, to appear).

De Sampaio, P. A. B. & Coutinho, A.L.G.A., 1999, Simulation of free and forced convection incompressible flows using an adaptive parallel/vector finite element procedure, International Journal for Numerical Methods in Fluids, vol. 29, 289-309.

Hirsch, C, 1988, Numerical Computation of Internal and External Flows, Vol. 1, John Wiley & Sons, New York.

Karki, K.C. & Patankar, S.V., 1989, Pressure based calculation procedure for viscous flows at all speeds in arbitrary configurations, AIAA Journal, vol. 27, pp. 1167-1174.

Maliska, C.R. & Silva, A.F.C., 1989, A boundary-fitted finite volume method for the solution of compressible and/or incompressible fluid flows using both velocity and density corrections, in Finite Elements in Fluids, eds. T.J. Chung and G. Karr, Huntsville Press.

Moreira, M.L., 1998, Simulação computacional de escoamentos viscosos compressíveis/ quase incompressíveis, D.Sc. Thesis, Programa de Engenharia Civil (COPPE/UFRJ), Rio de Janeiro, RJ, Brazil.

Nigro, N., Sorti, M. & Idelsohn, S., 1997, GMRES physics-based preconditioner for all Reynolds and Mach numbers: Numerical examples, International Journal for Numerical Methods in Fluids, vol. 25, 1347-1371.

Zienkiewicz, O.C. & Zhu, J.Z., 1987, A simple error estimator and adaptive procedure for practical engineering analysis, International Journal for Numerical Methods in Engineering, vol. 24, pp. 337-357.

Zienkiewicz, O.C. & Codina, R., 1995, A general algorithm for compressible and incompressible flow. part I: the split, characteristic-based scheme", International Journal for Numerical Methods in Fluids, vol. 20, 869-885.